Video Article

Human Brown Adipose Tissue Depots Automatically Segmented by Positron Emission Tomography/Computed Tomography and Registered Magnetic Resonance Images

Aliya Gifford[1], Theodore F. Towse[2], Ronald C. Walker[3], Malcolm J. Avison[4], E. Brian Welch[3]

[1]Chemical and Physical Biology Program, Vanderbilt University

[2]Department of Physical Medicine and Rehabilitation, Vanderbilt University School of Medicine

[3]Radiology & Radiological Sciences, Vanderbilt University Medical Center

[4]Department of Pharmacology, Vanderbilt University

Correspondence to: E. Brian Welch at brian.welch@vanderbilt.edu

URL: http://www.jove.com/video/52415
DOI: doi:10.3791/52415

Keywords: Medicine, Issue 96, magnetic resonance imaging, brown adipose tissue, cold-activation, adult human, fat water imaging, fluorodeoxyglucose, positron emission tomography, computed tomography

Date Published: 2/18/2015

Citation: Gifford, A., Towse, T.F., Walker, R.C., Avison, M.J., Welch, E.B. Human Brown Adipose Tissue Depots Automatically Segmented by Positron Emission Tomography/Computed Tomography and Registered Magnetic Resonance Images. *J. Vis. Exp.* (96), e52415, doi:10.3791/52415 (2015).

Abstract

Reliably differentiating brown adipose tissue (BAT) from other tissues using a non-invasive imaging method is an important step toward studying BAT in humans. Detecting BAT is typically confirmed by the uptake of the injected radioactive tracer ^{18}F-Fluorodeoxyglucose (^{18}F-FDG) into adipose tissue depots, as measured by positron emission tomography/computed tomography (PET-CT) scans after exposing the subject to cold stimulus. Fat-water separated magnetic resonance imaging (MRI) has the ability to distinguish BAT without the use of a radioactive tracer. To date, MRI of BAT in adult humans has not been co-registered with cold-activated PET-CT. Therefore, this protocol uses ^{18}F-FDG PET-CT scans to automatically generate a BAT mask, which is then applied to co-registered MRI scans of the same subject. This approach enables measurement of quantitative MRI properties of BAT without manual segmentation. BAT masks are created from two PET-CT scans: after exposure for 2 hr to either thermoneutral (TN) (24 °C) or cold-activated (CA) (17 °C) conditions. The TN and CA PET-CT scans are registered, and the PET standardized uptake and CT Hounsfield values are used to create a mask containing only BAT. CA and TN MRI scans are also acquired on the same subject and registered to the PET-CT scans in order to establish quantitative MRI properties within the automatically defined BAT mask. An advantage of this approach is that the segmentation is completely automated and is based on widely accepted methods for identification of activated BAT (PET-CT). The quantitative MRI properties of BAT established using this protocol can serve as the basis for an MRI-only BAT examination that avoids the radiation associated with PET-CT.

Video Link

The video component of this article can be found at http://www.jove.com/video/52415/

Introduction

Due to the marked rise in obesity worldwide, there is an increased interest in research areas aimed at understanding energy balance. Obesity can result in costly and devastating medical conditions such as diabetes, liver disease, cardiovascular disease and cancer, making it a significant area of concern for public health[1]. One area of research aimed at understanding the balance of energy intake versus energy expenditure is the study of brown adipose tissue or BAT. Although termed an adipose tissue, BAT differs from the more common white adipose tissue (WAT) in many ways[2]. The function of white adipocytes is to store triglycerides in a single large lipid vacuole per cell, and to release these triglycerides as a source of energy into the blood stream when needed. In a very different manner, the function of brown adipocytes is to produce heat. One mechanism by which this occurs is through exposure to cold. This causes an increase in sympathetic nervous system activity, which in turn activates BAT. When activated, brown adipocytes generate heat. To do so, they use the triglycerides contained in the many small lipid vacuoles per cell, and through the presence of uncoupling protein 1 (UCP1) in the abundant mitochondria, convert the triglycerides to metabolic substrates without the production of ATP, resulting in entropic loss as heat generation. As the triglycerides stored in the small lipid vacuoles are depleted, the adipocyte takes up both glucose and triglycerides present in the blood stream[3].

Interest in studying BAT has dramatically increased in recent years due to its contribution to non-shivering thermogenesis, its role in modulating the body's energy expenditure, and the potential inverse relationship between BAT and obesity[3–9]. In addition, recent animal studies indicate BAT plays a critical role in clearing triglycerides and glucose from the blood stream, especially following ingestion of a high fat meal[10,11]. However, most of what we know about BAT is a result of research in small mammals, which contain many depots of BAT[4,9,12–15]. Notwithstanding a few early studies[16–18], the presence of BAT in humans was widely thought to diminish with age until recently when interest in studying human BAT has been renewed. Recent research suggests that relatively small amounts of BAT persist into adulthood[19–24]. An additional limiting factor to studying BAT is that apart from biopsy and histological staining, the currently accepted unequivocal method for detecting BAT is ^{18}F-

fluorodeoxyglucose (^{18}F-FDG) positron emission tomography (PET). Modern PET scanners are typically combined with a computed tomography (CT) scanner. When activated by cold exposure, BAT takes up the ^{18}F-FDG radiotracer, which is a metabolic analogue of glucose, and becomes visible on PET images, in comparison to the much lower level of ^{18}F-FDG uptake when BAT is inactive[20,21,23,25]. CT images acquired during a PET exam on a PET-CT scanner help to differentiate between tissues with high ^{18}F-FDG uptake by providing anatomical information. This use of PET-CT imaging exposes the subject to ionizing radiation (predominately from PET, though the dose from the CT scan is not negligible), and is therefore an undesirable method for BAT detection.

Although the number of studies on BAT in healthy adult humans is increasing, recent studies of human BAT have mainly been limited to retrospective PET-CT studies[19,25], human infant cadavers[26,27], human adolescents who have already been admitted to hospitals for other reasons[27–30], and a few human studies of healthy adults[31–35]. One of the challenges with both studies of children and retrospective studies is the possibility of altered results when studying a patient population who is sick, which may affect BAT. Additionally, because glucose is not the preferred fuel source of BAT[36], PET studies may not always detect activated BAT, and therefore may underrepresent the presence of BAT. Another difficulty in studying BAT with biomedical imaging is related to performing image segmentation to define the boundaries of tissue depots. Currently, segmentation of BAT in human studies often relies on some degree of manual image segmentation and is therefore vulnerable to misidentification of BAT depots, as well as inter-rater variability.

Because of these challenges, reliable spatial mapping techniques that can distinguish BAT from WAT distributions, along with automated segmentation methods, would provide investigators with a powerful new tool with which to study BAT. Magnetic resonance imaging (MRI) has the capability for identification, spatial mapping, and volumetric quantification of BAT, and unlike existing hybrid PET-CT imaging approaches that include a radioactive dose for the imaged subject, MRI involves no ionizing radiation and can be used safely and repeatedly. The ability to identify and quantify BAT using MRI can have a dramatic positive impact on clinical endocrinology and the pursuit of new avenues of obesity research. Previous fat-water MRI (FWMRI) studies of BAT in both mice and humans show that the fat-signal-fraction (FSF) of BAT is in the range of 40-80% fat, whereas WAT is above 90% fat[15,26,27]. We therefore hypothesize that this quantitative FWMRI metric, in conjunction with other quantitative MRI metrics, can be used in future work to visualize and quantify BAT depots in humans. This would provide the research community with a powerful tool with which to study BAT's influence on metabolism and energy expenditure without the use of ionizing radiation.

Our research group has been studying BAT in adult humans for the past three years. Our first public presentation on the use of MRI to investigate suspected BAT in one adult human subject occurred in February 2012 at the International Society for Magnetic Resonance in Medicine (ISMRM) Fat-Water Separation Workshop in Long Beach, California[37]. Two months later, our group presented FSF values in suspected BAT in two adults at the 20th annual meeting of the ISMRM in April 2012 in Melbourne, Australia[38]. One year later at the 21st annual meeting of the ISMRM in April 2013 in Salt Lake City, Utah, the protocol described in this manuscript was used for the first (to the best of our knowledge) public presentation of MRI quantification of PET-confirmed BAT in adult human subjects[39]. Specifically, we presented evidence showing that the previously suspected BAT was confirmed to be activatable BAT using both cold-activated and thermoneutral ^{18}F-FDG PET-CT imaging. Since 2013, our cohort of healthy adult human subjects imaged with both MRI and PET/CT under thermoneutral and cold-activated conditions has expanded to more than 20 subjects with results most recently presented in February 2014 at the workshop "Exploring the Role of Brown Fat in Humans" sponsored by the NIH NIDDK[40]. Specifically, we reported FWMRI FSF and R_2* relaxation properties in regions of supraclavicular BAT confirmed by ^{18}F-FDG PET-CT in adult humans, with the BAT ROIs delineated using automated segmentation algorithms based on the cold-activated and thermoneutral PET-CT scans. Most recently we presented results of temperature mapping in ^{18}F-FDG PET-CT confirmed BAT in adult humans using advanced FWMRI thermometry[41,42].

The procedure presented here acquires both MRI and ^{18}F-FDG PET-CT scans on the same subject, each after exposure to both cold-activated and thermoneutral conditions. The cold-activated and thermoneutral ^{18}F-FDG PET-CT scans are used to create automatically segmented BAT regions of interest (ROIs), on a subject specific basis. These BAT ROIs are then applied to the co-registered MRI scans to measure the MRI properties in the PET-CT confirmed BAT.

A limitation of this protocol is that the air temperature used when exposing subjects to either the warm or cold stimulus is consistent for every subject. This is a limitation because the temperature at which each subject experiences feeling warm or chilled can be different. Therefore, by running a trial session during which the air temperature is adjusted to fit the individual's response, and then using these temperatures during the thermoneutral and cold-activation protocols, it could be possible to obtain better responses from the brown adipose tissue.

Protocol

NOTE: The local ethics committee of this institute approved this study, and all subjects provided written informed consent prior to participation. To be eligible for the study, subjects must fulfill the following requirements: no known diabetes mellitus; no use of beta blockers or anxiety medications, currently or in the past; does not smoke or chew tobacco products, currently or in the past; no more than 4 cups of caffeine each day; no more than 2 glasses of alcohol each day; and if female, not pregnant or breastfeeding.
NOTE: In this study, each participant undergoes four exams: two MRI and two PET-CT. Each exam is acquired on a different day, with each imaging modality performed under both thermoneutral 24.5 ± 0.7 °C (76.2 ± 1.3 °F), and cold 17.4 ± 0.5 °C (63.4 ± 0.9 °F) conditions. The scans are not scheduled in any particular sequence, helping to minimize any potential bias to the data due to heating or cooling the subject in a specific order. The total effective radiation dose for one PET-CT scan is 6.4 mSv (millisievert), and the radiologist on staff recommends a washout period of at least 24 hr between each scan.

1. General MRI Safety and Imaging Concerns

1. Because the main magnetic field in MRI machines is always on, take care to ensure the safety of the patient and all personnel working in the MR area. Clear all magnetic objects from the subject and any persons working in the area.
2. Ask subjects during the recruitment phase if they have any metal in their bodies[43]. In addition, have the subject complete a magnetic safety screening process[44] to ensure that any metal in the body is approved for MRI. This initial check can help eliminate the possibility of consenting a subject who cannot complete the MRI scan.

3. Additionally, if there is any metal in the subject's body, which is compatible with MR, ensure that the metal is not near the tissue of interest. This is because metal can cause image distortion artifacts, which will make the analysis difficult if not impossible.

2. Obtaining Informed Consent

1. Meet with the subject to obtain written informed consent. During this meeting, cover all details of the study, for example: the number of visits, the time commitment per visit, what the requirements are of the subject regarding limitations to exercise and/or food, what the subject can and cannot do during the visit (such as sleep), and any other specifics. Use this meeting to schedule the visits for the scanning, as it is usually easier to schedule these in person rather than using multiple emails.

3. Procedures Prior to Visit

1. Instructions for the Subject
    1. For 24 hr prior to arriving for the study, have the subject refrain from alcohol, caffeine, medication or any strenuous exercise or activity.
    2. Instruct the subject to fast and to avoid any caloric intake for 8 hr prior to arriving for the study. Subjects are allowed to drink water.

2. Contacting Volunteer
    1. Remind the volunteer of the specific instructions the day before the start of their 24 hr preparation. This serves both as a reminder of the scan, as well as it helps to ensure that the subject remembers their restrictions, (*i.e.*, no eating, no exercise, no alcohol, *etc*.).

4. Procedure on Study Day – for MRI

1. Temperature-Controlled Room Preparation
    1. Use a small room as the temperature-controlled room where the subject is exposed to the desired temperature.
    NOTE: By using a small room, it is possible to minimize temperature gradients in the room. For example, the room size used here is 7' x 6' 8" x 8' tall, (373.33 cubic feet).
    2. Prepare the room at least 60 min prior to the subject entering the room to allow sufficient time for the room to reach a stable temperature.
    3. Maintain the RT either with a portable air-conditioning unit and a rotating floor fan to keep the cool air circulating, or using a programmable portable heater, which oscillates to circulate the warm air around the room.
    4. Deactivate or minimize any existing thermostat controlling air-conditioning or heating of the room to avoid conflicting with the desired RT target of the portable devices.

2. Prior to Entering Temperature-Controlled Room
    1. Have the subject change into standard medical shorts and shirt. Remove socks and shoes. If the subject is female, allow the wearing of a sports bra that does not contain any metal.
    2. Measure the subject's height, weight, and waist circumference measurements after changing into the standard clothing.
    3. Measure the subject's body temperature using a sublingual thermometer.

3. In the Temperature-Controlled Room
    1. Direct the subject to enter the temperature-controlled room. Ask the subject to sit quietly and not perform any activity that could change body temperature, *e.g.*, exercising, typing, or falling asleep.
    2. After sitting in the room for 1 hr, measure the body temperature again using a sublingual thermometer.
    3. After the second hr of sitting in the temperature-controlled room, measure the body temperature again using a sublingual thermometer.
    4. On the MRI day when the subject is sitting in the cold room, use a cold vest to maintain a cold environment while the subject is transported to the MRI scanner. Place the cold vest on the subject prior to the subject leaving the temperature-controlled room.
    5. After 2 hr in the temperature-controlled room, transport the subject in a wheelchair to the MRI scanner. Use the wheelchair to keep the subject in a relaxed, sedentary state, and to minimize any "warming" that might occur from walking. Additionally, using the wheelchair helps to avoid any uptake of the PET tracer into skeletal muscles, though it would likely be minimal.

4. MRI Acquisition Protocol
    1. Acquire MRI scans using a 3T MRI scanner equipped with two-channel parallel transmit capability, an extra-large 16-channel torso receive coil, and a modified tabletop.
    2. Hang the anterior portion of the torso receive coil from the top of the scanner bore in a fabric sling. Allow the sling to hang low enough to slide against the subject's body in order to maximize signal-to-noise ratio (SNR).
    3. Place the posterior portion of the torso receive coil in a rolling "coil wagon" sandwiched between two layers of the tabletop. As the table moves through the scanner bore, hold the coil wagon at isocenter by straps attached to the scanner covers at the front and back of the scanner bore so that the posterior coil element remains stationary.
    4. Position the subject on the bed to enter the scanner feet first in a supine position.
        1. If the subject is wearing the cold vest, remove the vest prior to the subject lying down.
    5. Once lying down, have the subject place both arms inside a bag similar to a pillowcase, and lower the arms to either side of the body. This helps ensure the shoulders are positioned in a similar manner during both the MRI and PET/CT exams, which makes image co-registration easier.
    NOTE: Allowing the subject to lie down on the scanner bed naturally, using the same amount of cushioning under the head during each scan, and using the pillowcase bag to support the arms, all helps to minimize differences between subject positioning between scans. Any support used for the subject during one scan, for example a pillow under the knees or lower back, should always be used in the same way for that subject, during both the MRI and PET/CT scans.

6. Acquire fat-water MRI (FWMRI) using a multi-stack, multi-slice, multiple fast field echo (mFFE) acquisition with 7 stacks of 20 axial slices, covering from the crown of the head to upper thigh. Slices are contiguous with a 0 mm gap between slices.
    1. Collect FWMRI scans using customized software to enable the acquisition of 8 echoes acquired as two interleaved sets of four echoes with a TR = 83 ms, TE_1=1.024 ms and effective ΔTE = 0.779 ms. Other acquisition protocol details include: flip angle = 20º, water fat shift = 0.323 pixels, readout sampling bandwidth = 1346.1 Hz/pixel, axial in-plane field of view = 520 mm × 408 mm, acquired voxel size = 2 mm x 2 mm x 7.5 mm, and sensitivity encoding (SENSE) parallel imaging factor = 3 (anterior posterior direction). Preparation phases for each station include center frequency (F_0) optimization and first order linear shimming. Acquisition time is 27.8 sec for 20 slices.
    2. Perform breath holds for stations covering the pelvis to the shoulders with two breath holds per station, *i.e.*, no breath hold is longer than 14 sec. At each table position, acquire a dual angle B_1 calibration scan (acquisition time 15.1 sec) to enable optimized RF shimming (relative RF amplitude and phase adjustments) for the two-channel transmit capability of the scanner.
    3. Acquire a SENSE reference scan at each table position with an acquisition time of 12.1 sec. Recommended FWMRI parameters are listed in **Table 1**.

5. Procedure on Study Day – for PET-CT

1. Temperature-Controlled Room Preparation
    1. Use a small room as the temperature-controlled room where the subject is exposed to the desired temperature.
    NOTE: By using a small room, it is possible to minimize temperature gradients in the room. For example, the room size used here is 7' x 6' 8" x 8' tall, (373.33 cubic feet).
    2. Prepare the room at least 60 min prior to the subject entering the room to allow sufficient time for the room to reach a stable temperature.
    3. Maintain the RT either with a portable air-conditioning unit and a rotating floor fan to keep the cool air circulating to achieve the cold stimulus temperature, or using an oscaillating portable heater to maintain the thermoneutral temperature.
    4. Deactivate or minimize any existing thermostat controlling air-conditioning or heating of the room to avoid conflicting with the desired RT target of the portable devices.

2. Subject Preparation
    1. Direct the subject to the PET imaging suite to have an IV port placed in a hand or arm vein. This IV port allows the Radiology technician to inject the radiotracer later, when the subject is sitting in the temperature-controlled room.
    2. If the subject is female, perform a blood serum pregnancy test to ensure she is not pregnant.
    NOTE: For this study, the internal review board requires a pregnancy test less than 24 hr prior to the PET/CT scan being acquired.

3. Prior to Entering Temperature-Controlled Room
    1. Have the subject change into standard medical shorts and shirt. Remove socks and shoes. If the subject is female, allow the wearing of a sports bra that does not contain any metal.
    2. Measure the subject's height, weight, and waist circumference measurements after changing into the standard clothing.
    3. Measure the subject's body temperature using a sublingual thermometer.

4. In the Temperature-Controlled Room
    1. Direct the subject to enter the temperature-controlled room. Ask the subject to sit quietly and not perform any activity that could change body temperature, *e.g.*, exercising, typing, or falling asleep.
    2. After sitting in the room for 1 hr, measure the body temperature again using a sublingual thermometer.
    3. On the PET-CT scan days after the first hour in the temperature-controlled room, have a radiology technician administer the injection of Fluorodeoxyglucose (^{18}F-FDG) through the IV port. Inject 0.14 mCi/kg (approximately 10 mCi for a 70 kg subject) of ^{18}F-FDG. Calculate exact dosage based on subject specific weight.
    4. After the second hr of sitting in the temperature-controlled room, measure the body temperature again using a sublingual thermometer.
    NOTE: Unlike the cold MRI days, use of the cold vest is unnecessary on cold PET-CT days because the ^{18}F-FDG tracer is taken up into the activated BAT during the hour post tracer injection. The tracer will not leave the tissue even if the subject becomes warm as he/she is being transported to the scanner. Therefore, because it is possible to detect the presence of activated BAT on the PET-CT images even if the BAT does not remain active during the PET-CT scan, the cold vest is not necessary.
    5. After 2 hr in the temperature-controlled room, transport the subject in a wheelchair to the PET-CT scanner. Use the wheelchair to keep the subject in a relaxed, sedentary state, and to minimize any "warming" that might occur from walking. Additionally, using the wheelchair helps to avoid any uptake of the PET tracer into skeletal muscles, though it would likely be minimal.

5. PET-CT Acquisition Protocol
    1. Acquire PET-CT scans on a Discovery STE PET/CT scanner (STE stands for See and Treat Elite).
    2. Position the subject on the bed to enter the scanner head first in a supine position.
    3. Once lying down, have the subject place both arms inside a bag similar to a pillowcase, and lower the arms to either side of the body. This helps ensure the shoulders are positioned in a similar manner during both MRI and PET/CT exams, which makes image co-registration easier.
    NOTE: The PET/CT imaging field of view covers from the crown of the head to mid-thigh in 7-9 bed positions, depending on subject height (2 min per bed position). Recommended PET-CT parameters are listed in **Table 2**.

6. MRI Post Processing

1. Save real and imaginary MR images for off-line processing.The signal measured by MRI is a vector quantity with both magnitude and direction that can be represented as a complex number with real and imaginary parts. In the clinical setting, the magnitude images are typically displayed. However, complex information is needed for processing into the fat and water images.
2. Perform three-dimensional water/fat separation and R_2* estimation based on a multi-scale whole-image optimization algorithm[45] implemented in C++ for each individual slice stack. Fat is modeled using 9 peaks[46].
3. Discard the first echo of each 4-echo train to avoid potential contamination of eddy current in the complex water-fat signal model.

7. PET-CT Post Processing

1. Load CT DICOM data into MATLAB and convert to Hounsfield units (HU) by applying the scanner-supplied rescale value to the data values.
2. Load PET DICOM data into MATLAB and convert to Standardized Uptake Values (SUV) using the following formula:

$$SUV = \frac{(pixel\ value) * (subject\ weight\ [grams])}{actual\ activity}$$

where “pixel value” is the stored value in the DICOM file for that pixel location.

$$actual\ activity = (PET\ tracer\ activity) * 2^{\frac{-time\ elapsed}{(PET\ tracer\ half-life)}}$$

NOTE: The PET tracer activity is the radionuclide total dose, and can be read from the image meta-data (DICOM header file).

$$time\ elapsed = (scan\ time) - (injection\ time)\ [minutes]$$

3. Interpolate the PET data to have the same dimensions as the CT data.
    1. Because PET and CT images are acquired with the same slice thickness, perform interpolation using a 2-dimensional spline function in the X-Y plane.

8. Data Post Processing

1. To analyze the images, co-register all 4 image-volumes for each subject using a rigid body registration algorithm[47] via a semi-automated method with in-house developed 3-plane view software to verify registration in all three dimensions.
2. Due to difficulties with registering the entire image volume across all four time-points, focus registration on the region covering the neck to the apex of the lungs. Use only the successfully registered region in further data processing.
3. Following image registration, load FWMRI, CT HU and PET SUV data into MATLAB and use to define BAT regions of interest.
   NOTE: Similar to previously published methods[19,25,48] of distinguishing BAT using PET SUV and CT HU values, to be considered part of the BAT mask, each voxel in the image must satisfy the following: (1) HU value falls in the range of: -200 < HU < -1, on both cold and warm CT scans; (2) SUV > 2.0 on the cold PET scan; (3) SUV signal fraction [(Cold SUV)/(Cold SUV + Warm SUV)] > 0.55, *i.e.*, the cold PET scan must generate more than 55% of the total observed SUV signal in that voxel; and (4) only contain foreground pixels from the MRI scan, where Otsu’s method[49] is used to classify foreground pixels.
4. If a voxel fulfills all these criteria, include the voxel in the binary mask of BAT identity.
5. Apply the following binary morphology steps.
    1. Create a matrix the same size as the images being processed. Each spatial location in the new matrix is the 3D sum of all its adjacent neighbors in the binary BAT mask, including diagonals. The maximum sum is 26.
    2. Threshold this new matrix to include only locations with 15 or more 3D neighbors. This matrix then forms the final binary BAT mask.
       NOTE: These rules are sufficient to segment BAT tissue, and no further modification to the mask is necessary to eliminate non-BAT voxels. This forms a slice-by-slice mask of PET-CT confirmed BAT in the co-registered shoulder region.
6. Apply the mask to all the co-registered images to acquire the SUV, HU, fat signal fraction (FSF) and R_2* values in the BAT regions, for both the cold and warm scans.

Representative Results

Acquiring both MRI and PET-CT scans on the same subject, and performing co-registration on all scans enables reliable measurement of quantitative MRI metrics of BAT. **Figure 1** shows the unprocessed warm (TN) and cold (CA) PET-CT and MRI scans from one subject. By acquiring both TN and CA PET-CT data, it is possible to clearly distinguish the cold-activated BAT depots by the increased ^{18}F-FDG uptake. After co-registering all four scans **(Figure 2** and **3)**, it is possible to create a subject-specific BAT mask using criteria derived from the PET-CT images, as seen in **Figure 4**. This mask can then be applied to the four co-registered scans to acquire image metrics in the BAT depots. Representative values from one subject are displayed in **Table 1**.

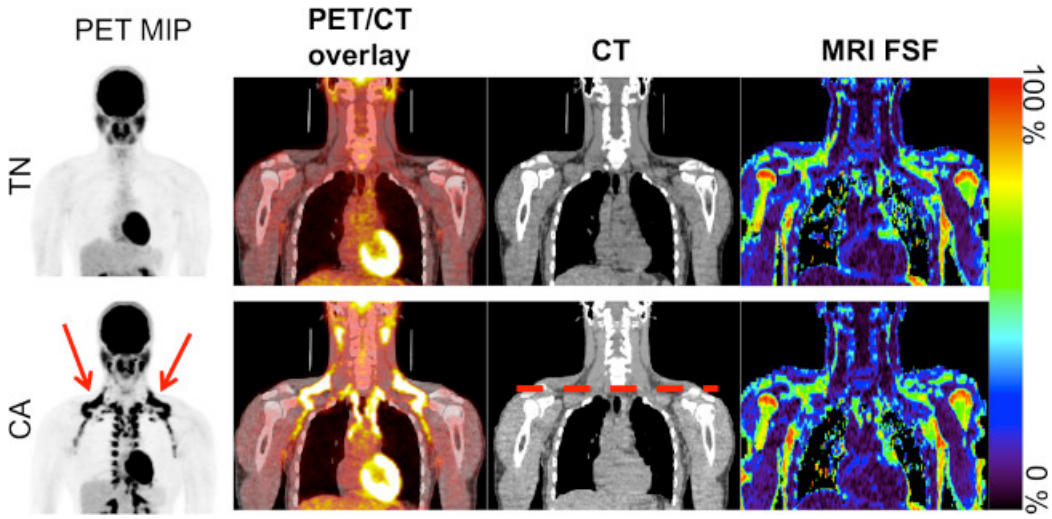

Figure 1. Coronal images from the warm (TN) and cold (CA) scans for one subject showing the PET maximum intensity projection (MIP) in inverse gray scale, PET/CT overlay, CT, and MRI fat signal fraction (FSF). Note the increased ^{18}F-FDG uptake in the clavicular region (red arrow), as well as down the spinal column on the CA PET MIP scan, indicating activated brown adipose tissue. The dashed red line on the CA CT image indicates the clavicular region to be further analyzed. Please click here to view a larger version of this figure.

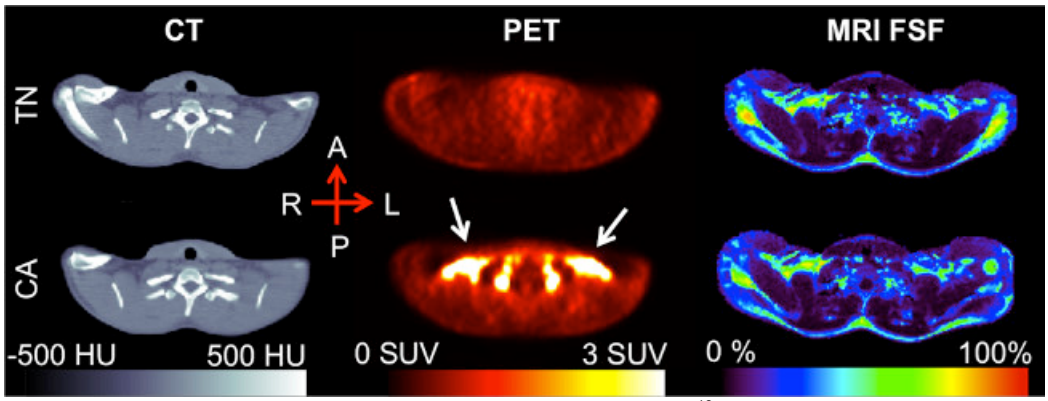

Figure 2. Clavicular-level axial slice, post-registration. The increased ^{18}F-FDG uptake seen in the CA PET scan (white arrows), occurs in the supraclavicular region of adipose tissue as determined by the CT Hounsfield Unit values. The MRI fat signal fraction (FSF) in this region falls in the 50-80% range, similar to that of previous research. Please click here to view a larger version of this figure.

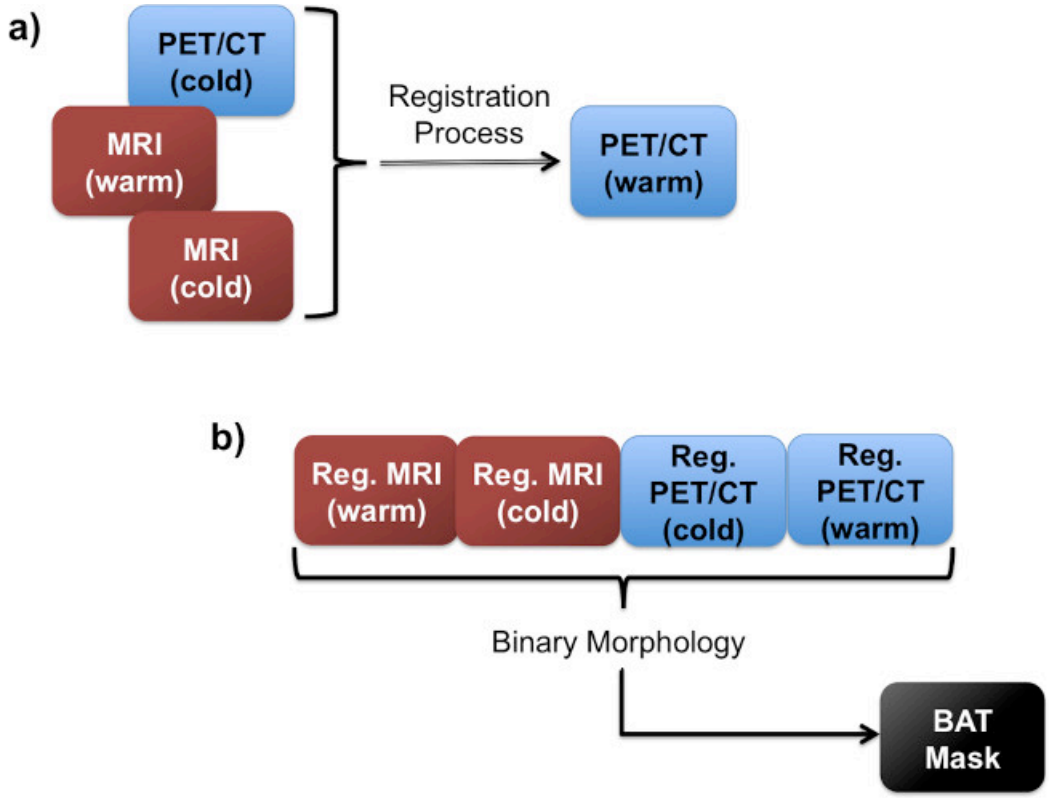

Figure 3. Flow charts showing the registration step. (A), in which the images are all registered to the same image space. Following the registration, all four images are used in the BAT mask creation **(B)**.

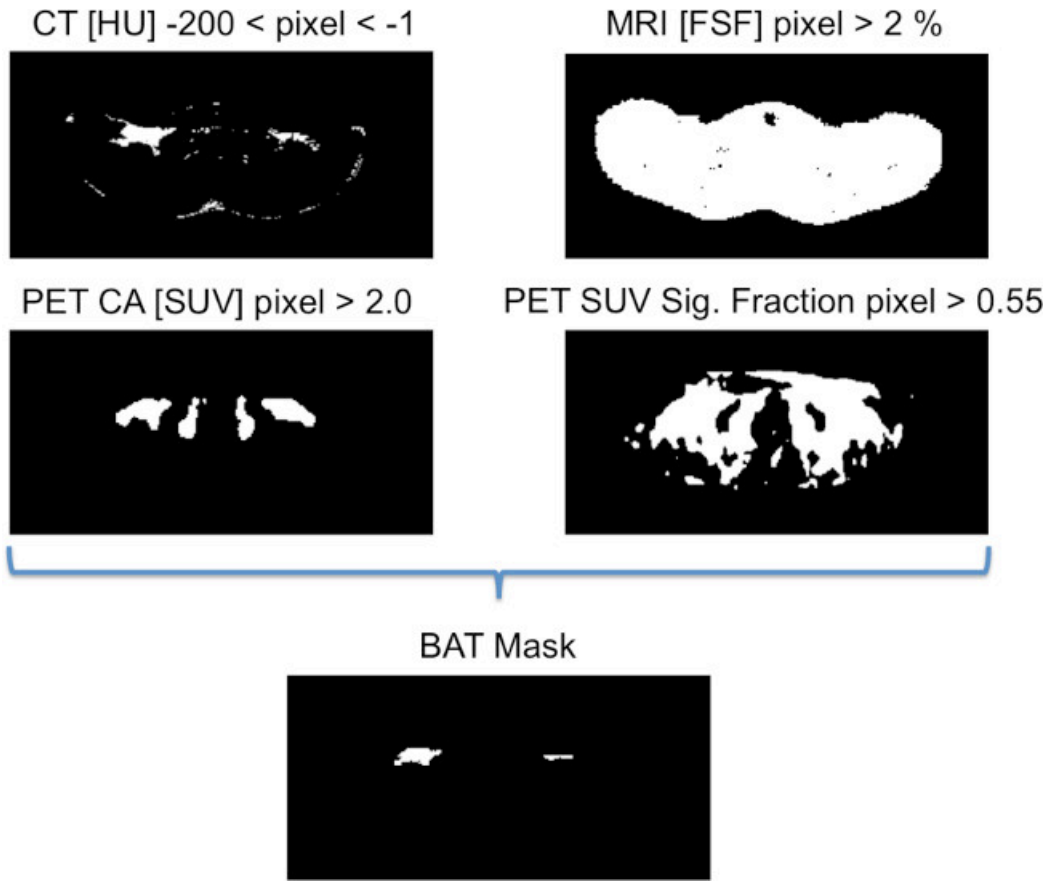

Figure 4. Binary images showing the criteria for generating the BAT mask. To be considered part of the BAT mask, each voxel in the image must satisfy these four rules, as determined on a slice-by-slice basis. If a voxel fulfills all these criteria, it is included in the binary mask of BAT identity. Please click here to view a larger version of this figure.

Imaging Method	**Value:**
	Mean ± 95% C.I.
Thermoneutral CT [HU]	-68.62 ± 9.35
Cold-Activated CT [HU]	-55.04 ± 7.72
Thermoneutral PET [SUV]	0.52 ± 0.05
Cold-Activated PET [SUV]	7.15 ± 1.16
Thermoneutral FSF [%]	41.62 ± 5.04
Cold-Activated FSF [%]	47.76 ± 5.15
Thermoneutral R2* [1/sec]	128.22 ± 19.48
Cold-Activated R2* [1/sec]	101.27 ± 24.92

Table 1. Numerical values (mean 95% Confidence Interval) from both the cold-activated and thermoneutral scans for one subject.

	Parameter	Recommendation
General	Sequence type	Multi-echo Fast Field Echo (mFFE)
	RF transmission coil	Quadrature-body
	Receive coil	SENSE-XL-Torso
	Total scan duration (min:sec)	00:25 (per table station)
Geometry	Multi-transmit	Yes
	Anatomical plane	Transverse
	Number of slices	20
	Slice thickness (mm)	7.5
	Inter-slice gap (mm)	0
	Acquired Matrix	260 x 204
	Reconstruction matrix	288
	Field of view (mm)	520 x 408
	Reconstructed voxel size (mm)	1.81 x 1.82 x 7.5
	SENSE	Yes
	P reduction (AP)	3
	Slice scan order	Ascend
	Fold-over direction	Anterior-Posterior
	Fat shift direction	Left
Contrast	Scan mode	Multi-slice
	Repetition time (ms)	83
	Echoes	4
	Interleaved mFFE	Yes
	Interleaved count	2
	Echo time (first) (ms)	1.023
	Echo time spacing (ms)	1.559
	Effective interleaved echo time (ms)	0.7793
	Excitation flip angle (°)	12
	RF shimming	Adaptive
Signal acquisition	Parallel imaging	SENSE factor = 3
	Partial Fourier	No
	Bandwidth/pixel (Hz/pixel)	1346.1

Table 2. Parameters used for fat-water MRI (FWMRI) acquisition.

Parameter	Recommendation
Acquisition mode	Helical
Data collection diameter (mm)	500
Reconstruction diameter (mm)	700
Exposure time (seconds)	873
Convolution kernel	Standard
Revolution time (sec)	0.8
Single collimation width (mm)	1.25
Spiral pitch factor	1.675
Field of view – CT	512 x 512
Field of view – PET	128 x 128
Slice thickness (mm)	3.75
Reconstructed voxel size (mm) – CT	1.37 x 1.37 x 3.75
Reconstructed voxel size (mm) – PET	5.47 x 5.47 x 3.75
Total number of slices	299 - 335

Table 3. Parameters used for PET-CT image acquisition.

Discussion

The described study protocol is designed to use both thermoneutral and cold-activated PET/CT to automatically segment BAT depots on a subject specific basis. These automatically generated regions of interest can then be applied to both thermoneutral and cold-activated MRI scans which have been co-registered to the PET/CT scans of the same subject. To the best of our knowledge, this is the first research to perform both MRI and PET/CT after thermoneutral and cold-activated conditions on the same healthy adult human volunteer. The procedure described here requires four visits, with one imaging session performed on each day. Through further analysis using this method, it would be possible to determine precise MRI properties of brown adipose tissue in adult humans using PET-confirmed regions of interest. This would enable future studies to detect and quantify the BAT in humans potentially using only MRI. Unlike PET, which is the current defacto gold standard of imaging BAT, the ability to image BAT using MRI would avoid radiation exposure. Additionally, MRI-based studies of BAT involving pediatric subjects as well as longitudinal studies would not involve radiation exposure. Because BAT is more often observed in leaner individuals and is inversely correlated with other metabolic syndrome indices, it is possible that increasing BAT mass and or activity may counteract obesity[3,6,8,9,11,48,50,51]. Therefore, the ability to non-invasively detect and quantify BAT could lead to a better understanding of the role BAT plays in obesity and metabolism. Future MRI-based approaches could be used in longitudinal studies to assess interventions, *e.g.*, pharmacological, dietary, or based on physical activity, used to increase the amount or activity of BAT.

One of the critical steps of this protocol is to obtain accurate registration of the imaging volumes. It is through the registration of the images that the BAT ROIs are produced; therefore image registration is key. Because ^{18}F-FDG uptake in PET images is diffuse due to the relatively large voxel size of PET imaging compared to MRI, it is important to use both PET SUV and CT HU values when creating the BAT ROI mask. Additionally, by using data from both thermoneutral and cold-activated conditions, it is possible to define the regions of ^{18}F-FDG uptake in the cold-activated scans which have more than 55% uptake compared to the thermoneutral conditions. This SUV signal fraction rule is necessary to eliminate tissues with a similarly high SUV on both the cold and thermoneutral scans. This helps limit the BAT ROI mask to only contain BAT regions, as the areas in the cold-activated scan with approximately equal levels of ^{18}F-FDG uptake as in the thermoneutral scan are ignored. Additionally, using the 15-pixel neighborhood rule is intended to capture regions that have a majority of BAT neighbors. The tradeoff is that low numbers will avoid eliminating small regions and eroding edges, while potentially leaving spurious voxels that are not BAT, and high numbers will erode boundaries and eliminate small BAT regions. While this method produces masks of brown adipose tissue, it does not claim to accurately capture the full BAT amount.

One of the downsides to this research protocol is the “one-size-fits-all” approach to both warming and cooling the subjects. Future work would benefit from using a more individualized approach to maximize non-shivering thermogenesis, and therefore maximize the BAT activation, for each subject. Additionally, heating the subject to a thermoneutral condition could benefit from using a subject-specific temperature, ensuring that the BAT is no longer in an active state on an individualized basis. The benefit of using individualized cooling protocols was emphasized in the recent publication by van der Lans *et al.*[52], and is a key potential modification to improve this protocol. Additionally, absent from this protocol is that there were no attempts made to determine menstrual cycle status in the female subjects. This could easily be corrected for in future studies.

Disclosures

The authors declare that they have no competing financial interests or other conflicts of interests.

Acknowledgements

We would like to thank the Vanderbilt University Institute of Imaging Science MRI technologists David Pennell, Leslie McIntosh, and Kristen George-Durrett, and the team of Vanderbilt University Medical Center PET/CT technologists led by Martha D. Shone. This work was supported by the following grants from the NIH: NCATS/NIH UL1 RR024975, NIDDK/NIH R21DK096282, NCI/NIH R25CA136440, and NIBIB/NIH T32EB014841.

References

1. Eckel, R. H., Alberti, K. G. M. M., Grundy, S. M., Zimmet, P. Z. The metabolic syndrome. *Lancet.* **375**, (9710), 181-183 (2010).
2. Cinti, S. Between brown and white: novel aspects of adipocyte differentiation. *Annals of Medicine.* **43**, (2), 104-115 (2011).
3. Stephens, M., Ludgate, M., Rees, D. A. Brown fat and obesity: the next big thing. *Clinical Endocrinology.* **74**, (6), 661-670 (2011).
4. Cannon, B., Brown Nedergaard, J. adipose tissue: function and physiological significance. *Physiological Reviews.* **84**, (1), 277-359 (2004).
5. Yoneshiro, T. Age-related decrease in cold-activated brown adipose tissue and accumulation of body fat in healthy humans. *Obesity (Silver Spring, Md).* **19**, (9), 1755-1760 (2011).
6. Seale, P., Lazar, M. a Brown fat in humans: turning up the heat on obesity). *Diabetes.* **58**, (7), 1482-1484 (2009).
7. Van Marken Lichtenbelt, W. Human brown fat +and obesity: methodological aspects. *Frontiers In Endocrinology.* **2**, (October), 52 (2011).
8. Frühbeck, G., Becerril, S., Sáinz, N., Garrastachu, P., García-Velloso, M. J. BAT: a new target for human obesity. *Trends in Pharmacological Sciences.* **30**, (8), 387-396 (2009).
9. Himms-Hagen, J. Thermogenesis in brown adipose tissue as an energy buffer. Implications for obesity. *New England Journal of Medicine.* **311**, (24), 1549-1558 (1984).
10. Bartelt, A. Brown adipose tissue activity controls triglyceride clearance. *Nature Medicine.* **17**, (2), 200-205 (2011).
11. Nedergaard, J., Bengtsson, T., Cannon, B. New powers of brown fat: fighting the metabolic syndrome. *Cell Metabolism.* **13**, (3), 238-240 (2011).
12. Kirov, S. A., Talan, M. I., Engel, B. T. Sympathetic outflow to interscapular brown adipose tissue in cold acclimated mice. *Physiology & Behavior.* **59**, (2), 231-235 (1996).
13. Guerra, C., Koza, R. A., Yamashita, H., Walsh, K., Kozak, L. P. Emergence of brown adipocytes in white fat in mice is under genetic control. Effects on body weight and adiposity. *Journal of Clinical Investigation.* **102**, (2), 412-420 (1998).
14. Kawate, R., Talan, M. I., Engel, B. T. Sympathetic nervous activity to brown adipose tissue increases in cold-tolerant mice. *Physiology & Behavior.* **55**, (5), 921-925 (1994).
15. Hu, H. H., Smith, D. L., Nayak, K. S., Goran, M. I., Nagy, T. R. Identification of brown adipose tissue in mice with fat-water IDEAL-MRI. *Journal of Magnetic Resonance Imaging.* **31**, (5), 1195-1202 (2010).
16. Heaton, J. M. The distribution of brown adipose tissue in the human. *Journal of Anatomy.* **112**, (Pt 1), 35-39 (1972).
17. Tanuma, Y., Tamamoto, M., Ito, T., Yokochi, C. The occurrence of brown adipose tissue in perirenal fat in Japanese). *Archivum histologicum Japonicum = Nihon soshikigaku kiroku.* **38**, (1), 43-70 (1975).
18. Huttunen, P., Hirvonen, J., Kinnula, V. The occurrence of brown adipose tissue in outdoor workers. *European Journal Of Applied Physiology And Occupational Physiology.* **46**, (4), 339-345 (1981).
19. Cohade, C., Osman, M., Pannu, H. K., Wahl, R. L. Uptake in supraclavicular area fat ("USA-Fat"): description on 18F-FDG PET/CT. *Journal of Nuclear Medicine Official Publication, Society Of Nuclear Medicine.* **44**, (2), 170-176 (2003).
20. Virtanen, K. A. Functional brown adipose tissue in healthy adults. *New England Journal of Medicine.* **360**, (15), 1518-1525 (2009).
21. Van Marken Lichtenbelt, W. D. Cold-activated brown adipose tissue in healthy men. *New England Journal of Medicine.* **360**, (15), 1500-1508 (2009).
22. Zingaretti, M. C., Crosta, F., Vitali, A., Guerrieri, M., Frontini, A., Cannon, B. The presence of UCP1 demonstrates that metabolically active adipose tissue in the neck of adult humans truly represents brown adipose tissue. *Journal of the Federation of American Societies for Experimental Biology.* **23**, (9), 3113-3120 (2009).
23. Saito, M. High incidence of metabolically active brown adipose tissue in healthy adult humans: effects of cold exposure and adiposity. *Diabetes.* **58**, (7), 1526-1531 (2009).
24. Nedergaard, J., Bengtsson, T., Cannon, B. Unexpected evidence for active brown adipose tissue in adult humans. *American Journal of Physiology. Endocrinology and Metabolism.* **293**, (2), E444-E452 (2007).
25. Cypess, A. M. Identification and importance of brown adipose tissue in adult humans. *New England Journal of Medicine.* **360**, (15), 1509-1517 (2009).
26. Hu, H. H., Tovar, J. P., Pavlova, Z., Smith, M. L., Gilsanz, V. Unequivocal identification of brown adipose tissue in a human infant. *Journal of Magnetic Resonance Imaging.* **35**, (4), 938-942 (2012).
27. Hu, H. H., Perkins, T. G., Chia, J. M., Gilsanz, V. Characterization of human brown adipose tissue by chemical-shift water-fat MRI. *AJR. American Journal Of Roentgenology.* **200**, (1), 177-183 (2013).
28. Ponrartana, S., Hu, H. H., Gilsanz, V. On the relevance of brown adipose tissue in children. *Annals of the New York Academy of Sciences.* 1-6 (2013).
29. Chalfant, J. S. Inverse association between brown adipose tissue activation and white adipose tissue accumulation in successfully treated pediatric malignancy. *The American Journal Of Clinical Nutrition.* **95**, (5), 1144-1149 (2012).
30. Gilsanz, V., Smith, M. L., Goodarzian, F., Kim, M., Wren, T. aL., Hu, H. H. Changes in Brown Adipose Tissue in Boys and Girls during Childhood and Puberty. *Journal of Pediatrics.* 1-7 (2011).
31. Chen, Y. -C. I. Measurement of human brown adipose tissue volume and activity using anatomic MR imaging and functional MR imaging. *Journal Of Nuclear Medicine Official Publication, Society Of Nuclear Medicine.* **54**, (9), 1584-1587 (2013).
32. Van Rooijen, B. D. Imaging Cold-Activated Brown Adipose Tissue Using Dynamic T2*-Weighted Magnetic Resonance Imaging and 2-Deoxy-2-[18F]fluoro-D-glucose Positron Emission Tomography. *Investigative Radiology.* **48**, (10), 1-7 (2013).
33. Vosselman, M. J. Brown adipose tissue activity after a high-calorie meal in humans. *The American Journal Of Clinical Nutrition.* **98**, (1), 57-64 (2013).

34. Chen, K. Y. Brown fat activation mediates cold-induced thermogenesis in adult humans in response to a mild decrease in ambient temperature. *The Journal of Clinical Endocrinology And Metabolism.* **98**, (7), E1218-E1223 (2013).
35. Van der Lans, A. A. J. J., *et al.* Cold acclimation recruits human brown fat and increases nonshivering thermogenesis. *The Journal Of Clinical Investigation.* **123**, (8), 3395-3403 (2013).
36. Ma, S. W., Foster, D. O. Uptake of glucose and release of fatty acids and glycerol by rat brown adipose tissue in vivo. *Canadian Journal Of Physiology And Pharmacology.* **64**, (5), 609-614 (1986).
37. Gifford, A. T1 and Fat-Water Fraction Measurements in an Adult Human: Possible Markers for Brown Adipose Tissue. *Proceedings of the International Society for Magnetic Resonance in Medicine: Workshop on Fat-Water Separation.* **20**, (1269), (2012).
38. Gifford, A. Preliminary Indication of Brown Adipose Tissue in Adult Humans Using Fat-Water MRI. *Proceedings of the International Society for Magnetic Resonance in Medicine.* **21**, (1520), (2013).
39. Gifford, A. Detection of Brown Adipose Tissue in an Adult Human Using Fat-Water MRI with Validation by Cold-activated PET. *Proceedings of the International Society for Magnetic Resonance in Medicine.* **21**, (1520), (2013).
40. Gifford, A., Welch, E. B. Fat-Water MRI Properties of Brown Adipose Tissue in Adult Humans Using Automated Depot Segmentation Based on Cold-Activated and Thermoneutral PET-CT. *NIH NIDDK Workshop on Exploring the Role of Brown Fat in Humans.* **15**, (2014).
41. Welch, E. B., Gifford, A., Towse, T. F. Phantom validation of temperature mapping using fat-water MRI with explicit fitting of water peak location. *Proceedings of the International Society for Magnetic Resonance in Medicine.* **22**, (3065), (2014).
42. Gifford, A., Towse, T. F., Avison, M. J., Welch, E. B. Temperature mapping in Human Brown Adipose Tissue Using Fat-Water MRI with Explicit Fitting of Water Peak Location. *Proceedings of the International Society for Magnetic Resonance in Medicine.* **22**, (275), (2014).
43. Shellock, F. G. *Reference Manual for Magnetic Resonance Safety, Implants and Devices 2014.* Biomedical Research Publishing Group (2014).
44. *MRIsafety Screening Form.* Available from: http://www.mrisafety.com/GenPg.asp?pgname=ScreeningForm (2015).
45. Berglund, at, Ahlström, J., H,, Kullberg, J. Model-based mapping of fat unsaturation and chain length by chemical shift imaging--phantom validation and in vivo feasibility. *Magnetic resonance in medicine official journal of the Society of Magnetic Resonance in Medicine / Society of Magnetic Resonance in Medicine.* **68**, (6), 1815-1827 (2012).
46. Hamilton, G. In vivo characterization of the liver fat 1H MR spectrum. *NMR in Biomedicine.* **24**, (7), 784-790 (2011).
47. Maes, F., Collignon, a, Vandermeulen, D., Marchal, G., Suetens, P. Multimodality image registration by maximization of mutual information. *IEEE Transactions On Medical Imaging.* **16**, (2), 187-198 (1997).
48. Ouellet, V. Outdoor temperature, age, sex, body mass index, and diabetic status determine the prevalence, mass, and glucose-uptake activity of 18F-FDG-detected BAT in humans. *Journal of Clinical Endocrinology and Metabolism.* **96**, (1), 192-199 (2011).
49. Otsu, N. A Threshold Selection Method from Gray-Level Histograms. *IEEE Transactions on Systems, Man, and Cybernetics.* **9**, (1), 62-66 (1979).
50. Yoneshiro, T. Recruited brown adipose tissue as an antiobesity agent in humans. *The Journal of Clinical Investigation.* **123**, (8), 3404-3408 (2013).
51. Farmer, S. R. Obesity: Be cool, lose weight. *Nature.* **458**, (7240), 839-840 (2009).
52. Van der Lans, A. aJ. J., *et al.* Cold-Activated Brown Adipose Tissue In Human Adults - Methodological Issues. *American Journal Of Physiology. Regulatory, Integrative And Comparative Physiology.* **31**, (0), (2014).

